Nephrol Dial Transplant (2010) 25: 1067–1078
doi: 10.1093/ndt/gfp611
Advance Access publication 26 November 2009

# Glomerular and proximal tubule cysts as early manifestations of *Pkd1* deletion

Ali K. Ahrabi[1,6], François Jouret[1], Etienne Marbaix[2], Christine Delporte[3], Shigeo Horie[4], Sharon Mulroy[5], Catherine Boulter[5], Richard Sandford[5] and Olivier Devuyst[1]

[1]Division of Nephrology, Université catholique de Louvain Medical School, Brussels, Belgium [2]Division of Pathology, Université catholique de Louvain Medical School, Brussels, Belgium [3]Laboratory of Biological Chemistry and Nutrition, Université Libre de Bruxelles Medical School, Brussels, Belgium [4]Department of Urology, Teikyo University, Tokyo, Japan [5]Department of Medical Genetics, Cambridge Institute of Medical Research, Hills Road, Cambridge, UK and [6]Renal Division, Department of Medicine, Brigham and Women's Hospital and Harvard Medical School, Boston, MA 02115, USA

*Correspondence and offprint requests to*: Olivier Devuyst; E-mail: Olivier.Devuyst@uclouvain.be

## Abstract

**Background.** The homozygous deletion of *Pkd1* in the mouse results in embryonic lethality with renal cysts and hydrops fetalis, but there is no precise data on the segmental origin of cysts and potential changes associated with polyhydramnios.

**Methods.** We used *Pkd1*-null mice to investigate cystogenesis and analyze the amniotic fluid composition from embryonic day 12.5 (E12.5) to birth ($n$ = 257 embryos).

**Results.** Polyhydramnios was consistently observed from E13.5 in $Pkd1^{-/-}$ embryos, in absence of placental abnormalities but with a significantly higher excretion of sodium and glucose from E13.5 through E16.5, and increased cyclic adenosine 3'5-monophosphate (cAMP) levels at E14.5 and E15.5. The $Pkd1^{-/-}$ embryos started to die at E13.5, with lethality peaking at E15.5, corresponding to the onset of cystogenesis. The first cysts in $Pkd1^{-/-}$ kidneys emerged at E15.5 in mesenchyme-derived segments at the cortico-medullary junction, with a majority of glomerular cysts and fewer proximal tubule cysts (positive for megalin). The cysts extended to ureteric bud-derived collecting ducts (positive for *Dolichos biflorus* agglutinin lectin) from E16.5.

**Conclusions.** These studies indicate that *Pkd1* deletion is associated with a massive loss of solutes (from E13.5) and increased cAMP levels (E14.5) associated with polyhydramnios. These abnormalities precede renal cysts (E15.5), first derived from glomeruli and proximal tubules and later from the collecting ducts, reflecting the expression pattern of *Pkd1* in maturing epithelial cells.

**Keywords:** cystogenesis; glomerular and proximal tubule cysts; low-molecular-weight protein; megalin; polyhydramnios

## Introduction

Autosomal dominant polycystic kidney disease (ADPKD) is one of the most prevalent monogenic disorders, leading to end-stage renal disease in approximately half of the affected patients [1]. ADPKD is caused by mutations of either *PKD1* or *PKD2*, the genes that encode polycystin-1 and polycystin-2, respectively. These two proteins, which are located in the primary cilium, interact *in vivo* to regulate the proliferation and differentiation of renal tubular cells via various signalling pathways [2]. *PKD1* and *PKD2* are widely expressed throughout different foetal and adult tissues, explaining why ADPKD can affect extrarenal tissues including the liver, the pancreas and the arteries. In ADPKD kidneys, cysts originate from a small number of nephrons and possess functional and molecular characteristics of various nephron segments [3].

During normal human nephrogenesis, *PKD1* mRNA is absent from the uninduced mesenchyma and the emerging ureteric bud. From 10 weeks, a strong *PKD1* signal appears in the first set of differentiated proximal tubules (PT) from their glomerular origin. From 10 to 24 weeks, the differentiated PT express high levels of *PKD1* mRNA. At week 15, a discrete *PKD1* expression is also detected in the distal nephron and ureteric bud branches, persisting at a moderate level during foetal life [4]. In mouse embryonic kidneys, *Pkd1* is not expressed in the ureteric bud and comma and S-shaped bodies, and weakly expressed in induced metanephric mesenchyme from embryonic Day 13.5 (E13.5), to increase intensely in differentiating PT from E15.5 [5]. Several mouse models carrying mutations in *Pkd1* have been reported. All *Pkd1* knockout (KO) embryos die *in utero* by developing massive polycystic kidney disease, hydrops fetalis and polyhydramnios [5–10]. Some models are also characterized by vascular fragility [7] and cardiovascular and skeletal development defects [5], suggesting that the type of mutation in *Pkd1* may influence the severity of the phenotype and the stage of lethality. Taken together, these studies showed that polycystin-1 does not play a major role in early nephrogenesis, as the latter is normal in *Pkd1* mutant embryos [5–7]. Instead, polycystin-1 may participate in epithelial cell differentiation and tubular extension in late nephrogenesis.

While previous studies pointed to the severe renal cystogenesis and extrarenal phenotype of *Pkd1* embryos, there

has been no detailed investigation of the time-course and segmental origin of the cysts. Early functional abnormalities in human ADPKD include impaired urinary concentrating capacity [1,2] and urinary excretion of PT markers [11]. However, the factors contributing to polyhydramnios in *Pkd1* KO mice, including potential abnormalities in the placenta [12], remain unknown. In this study, we used a mouse model with a targeted deletion of *Pkd1*, resulting in a *Pkd1*-null allele [9], to investigate daily survival and cystogenesis *in utero*, as well as placental morphology and amniotic fluid (AF) volume and composition. Our data show that the loss of *Pkd1* is associated with a massive loss of solutes from E13.5 along with increased cyclic adenosine 3'5-monophosphate (cAMP) levels in the AF. These functional abnormalities precede the renal cysts, which are first detected in mesenchyme-derived glomerulus and PT segments and later in the collecting ducts.

## Materials and methods

### *Pkd1 mice and in utero analyses*

Studies were conducted on a *Pkd1* mouse model that was obtained by targeting the exons 2 to 5 and part of the exon 6 of *Pkd1*, resulting in a null allele [9,13]. The original stock of mice (mixed 129/sv/C57BL/6J background) was later backcrossed (at least six generations) to the C57BL/6J background. Heterozygous *Pkd1* mice, aged 10–15 weeks, were crossed to generate homozygous $Pkd1^{-/-}$ embryos. The gestational age was dated by appearance of the vaginal plug on the morning after mating, and designated as Day 0.5 (E0.5). Pregnant mice were sacrificed by cervical dislocation, and a caesarean section was performed to remove the uterus intact. The uterus was dissected and the embryos were removed under sterile, RNase-free conditions. The survival rate was based on embryos displaying a body movement or heart beating under microscopic examination. The embryos were placed on ice-cold Petri dishes and dissected to aspirate the AF and to harvest the kidneys. The studies covered the embryonic days E12.5 to E18.5 among a total of 257 embryos. We also used $Pkd1^{del17-21\beta geo}$ mouse embryos to investigate the expression of *Pkd1* in early tubulogenesis [5]. All protocols complied with the National Research Council Guide for the Care and Use of Laboratory Animals and were approved by the local ethics committee.

### *Antibodies and markers*

Sheep polyclonal antibodies against megalin (a gift of Dr. P. Verroust, INSERM, Paris, France) and uromodulin (Biodesign Int., Saco, ME); goat polyclonal antibodies against PECAM-1 (CD31, Santa Cruz Biotechnology, Santa Cruz, USA); rabbit polyclonal antibodies against aquaporin-1 (AQP1) (Chemicon-Millipore, Billerica, MA), aquaporin-2 (AQP2) (Sigma, Saint Louis, MO) and podocin (P35, a gift of Dr. C. Antignac, INSERM); mouse monoclonal antibodies against polycystin-1 (7E12, Santa Cruz Biotechnology); and *Dolichos biflorus* agglutinin (DBA) lectin (Sigma) were used.

The rabbit polyclonal antibody, anti-leucine-rich repeats (LRR), was raised against the N-terminal LRR domain of polycystin-1. Rabbits were immunized with purified His-tagged LRR domain (amino acids 27–360) expressed as a bacterial fusion protein; and antibodies purified using protein-A agarose as previously described [14]. The specificity of the purified anti-LRR antibodies was confirmed by ELISA (not shown) and Western blot analysis against both the polycystin-1 N-terminal fusion protein and the recombinant polycystin-1 LRR (Suppl. Fig. 1). Previous studies have shown that the anti-LRR antibodies were able to immunoprecipitate the *in vitro* translated N-terminal half of polycystin-1, and that immunostaining was abolished with preadsorption of antibody with fusion protein [14].

### *Immunohistochemistry*

Embryonic kidney samples were fixed in 4% paraformaldehyde (Boehringer Ingelheim, Heidelberg, Germany) in 0.1 mol/L phosphate buffer, pH 7.4, prior to embedding in paraffin as described [13]. Six-micrometre sections were cut and stained with hematoxylin and eosin. Additional sections were incubated for 30 min with 0.3% hydrogen peroxide to block endogenous peroxidase. Following incubation with 10% normal serum for 20 min, sections were incubated for 45 min with the primary antibodies diluted in PBS containing 2% bovine serum albumin (BSA). After washing, sections were successively incubated with biotinylated secondary anti-immunoglobulin (Ig) G antibodies, avidin–biotin peroxidase and aminoethylcarbazole (Vectastain Elite, Vector Laboratories). The M.O. M. kit (Vector Laboratories) was used for mouse-derived antibodies. Sections were viewed under a Leica DMR coupled to a Leica DC300 digital camera (Leica, Heerbrugg, Switzerland). Kidney sections of both $Pkd1^{-/-}$ and $Pkd1^{+/+}$ embryos ranging from E13.5 to E18.5 ($n = 4$ per embryonic day) were examined.

### *Staining for β-galactosidase activity in $Pkd1^{del17-21\beta geo}$ kidneys*

Staining for β-galactosidase activity in frozen tissue sections was carried out as previously described [5]. Tissues were fixed in X-gal fixative (0.2% paraformaldehyde (PFA), 0.1 M PIPES buffer, 2 mM $MgCl_2$, 0.1 M EGTA, pH 7.3) at 4ºC and cryoprotected in 30% sucrose/2 mM $MgCl_2$ before being snap frozen on $LN_2$ and stored at −160ºC in $LN_2$ until sectioned. Fifteen-micrometre tissue sections were fixed at 4°C for 10 min in X-gal fixative and rinsed briefly in ice-cold PBS/2 mM $MgCl_2$. The sections were permeabilized by washing in detergent rinse (0.1 M phosphate buffer, pH 7.3, 2 mM $MgCl_2$, 0.01% sodium deoxycholate, 0.02% NP-40) at 4ºC for 30 min, and stained in X-Gal staining solution (1mg/ml X-gal, 0.1 M phosphate buffer pH 7.3, 2 mM $MgCl_2$, 0.01% sodium deoxycholate, 0.02% NP-40, 5 mM potassium ferricyanide and 5 mM potassium ferrocyanide) at 37°C overnight in the dark. Stained sections were washed twice in PBS/2 mM $MgCl_2$, rinsed in $H_2O$ and counterstained for 2 min with nuclear fast red (Vector Laboratories). The sections were rinsed in water for 10 min, dehydrated with 5-min exchanges through graded methanol (50%, 70%, 90% and 100%) and cleared in Histoclear (Fischer Chemicals). Sections were mounted using Vectamount (Vector Laboratories).

### *Morphometric analyses of the placenta*

Volumic density of four different compartments of the placenta (the chorionic plate with stem villi, the labyrinth, the spongiotrophoblast and the giant cells) was determined by point counting, using a GF Planachromat 12.5× objective on a Jenamed 2 microscope (Jena, Jena, Germany) equipped with GF-PW 10× oculars containing a 100 crosses grid. A random whole histological cross-section was analysed for six placentas from $Pkd1^{+/+}$ and $Pkd1^{-/-}$ embryos at E13.5 by a pathologist unaware of the mouse genotype.

### *Analyses of AF*

The AF samples were prospectively collected from live embryos of pregnant $Pkd1^{+/-}$ females from E12.5 to E18.5. Each embryo was placed inside a pre-weighed chamber before inserting a BD Micro-Fine Insulin needle, 29 G × 12.7 mm, into the amniotic sac for AF aspiration. After careful aspiration, the foetal membrane was ruptured and opened up completely in order to collect all the remaining fluid. The total volume of the AF was measured in pre-weighed sterile tubes (intra-assay error <5%). Aliquots of AF were obtained at the time of aspiration and stored at −20°C. The concentrations of sodium and glucose were measured with Synchron CX5 PRO analyser (Beckman Coulter, Fullerton, CA). The concentrations of the low-molecular-weight (LMW) protein CC16 (Clara cell protein 16 kD) was determined using a sensitive radioimmunoassay as described [15].

### *cAMP measurement*

For cAMP measurement, AF (30 µl) was mixed with 300 µl of absolute ethanol, vortexed and centrifuged at 3500 *g* for 20 min at 4°C. The supernatant was collected and lyophilized using a Speed-Vac concentrator. cAMP levels were determined using a cAMP [$^{125}$I] Biotrak Assay (Amersham, Buckinghamshire, UK) following the acetylation procedure described in the assay. The lyophilized AF samples and cAMP standards (ranging from 2 to 128 fmol/100 µl) were submitted to acetylation by the addition of a mixture of acetic anhydride triethylamine (1:2; v:v).

**Table 1.** Survival rate of *Pkd1*-mutant embryos

| Crossed mice *n* | Embryonic Age | $Pkd1^{-/-}$ *n*: A (D) | $Pkd1^{+/+}$ *n*: A (D) | $Pkd1^{+/-}$ *n*: A (D) | Total embryos *n* |
|---|---|---|---|---|---|
| 2 | E12.5 | 3 (0) | 3 (0) | 12 (0) | 18 |
| 5 | E13.5 | 9 (1) | 6 (0) | 12 (0) | 28 |
| 6 | E14.5 | 12 (0) | 9 (0) | 17 (0) | 38 |
| 7 | E15.5 | 10 (4) | 11 (0) | 19 (0) | 44 |
| 5 | E16.5 | 5 (8) | 10 (0) | 16 (0) | 39 |
| 5 | E17.5 | 3 (8) | 8 (0) | 13 (0) | 32 |
| 5 | E18.5 | 3 (9) | 9 (0) | 15 (0) | 36 |
| 4 | At birth | 0 (4) | 6 (0) | 13 (0) | 23 |

A, alive; D, dead; n, number.

A duplicate of 100 µl aliquots from all standards and samples was pipetted into polypropylene tubes, then 100 µl of antiserum (except in tubes for the determination of non-specific), and 100 µl of cAMP [$^{125}$I] were added into all tubes, prior to being vortexed, and finally incubated for 4 h at 4°C. After the incubation, 500 µl of Amerelex-M secondary antibody reagent was added to each tube. The tubes were vortexed and then incubated for 10 min at room temperature. The antibody-bound fraction was separated by centrifugation at 2500 *g* for 15 min, and the supernatant liquid was discarded by careful aspiration. The radioactivity was counted in duplicate for 2 min in a gamma counter.

### *Data analysis*

Comparisons between groups were performed using two-tailed unpaired Student's *t*-test (GraphPad, San Diego, CA). Significance level was $P < 0.05$.

## Results

### *Survival rate and polyhydramnios in $Pkd1^{-/-}$ embryos*

Embryonic lethality was observed in $Pkd1^{-/-}$ embryos as early as E13.5, with a survival rate that sharply declined at E15.5. Only 25% (3/12) of $Pkd1^{-/-}$ embryos survived at E18.5, and none at birth. By contrast, all wild-type and heterozygous *Pkd1* embryos survived to birth (Table 1). The first abnormality found in $Pkd1^{-/-}$ embryos was the polyhydramnios, consistently observed from E13.5 (Figure 1A–C). The time-course analysis revealed a progressive and continuous increase in the total AF volume in $Pkd1^{-/-}$ mice, contrasting with the stability observed between E12.5 and E17.5 in both wild-type and heterozygous mice. The AF volume was significantly higher at all time points from E13.5 to E18.5 in $Pkd1^{-/-}$ vs. both $Pkd1^{+/+}$ and $Pkd1^{+/-}$ embryos (Figure 1D).

### *Histological analysis of the Pkd1-mutant placentas*

As abnormalities of the placental labyrinth layer have been described in a $Pkd1^{-/-}$ mouse model (K. Piontek *et al.*, unpublished work [12]), we performed a detailed morphometry analysis of the placentas of *Pkd1* mice at E13.5, the first stage associated with polyhydramnios. This analysis showed that the volumic density of each placental compartment was similar between $Pkd1^{+/+}$ and $Pkd1^{+/-}$

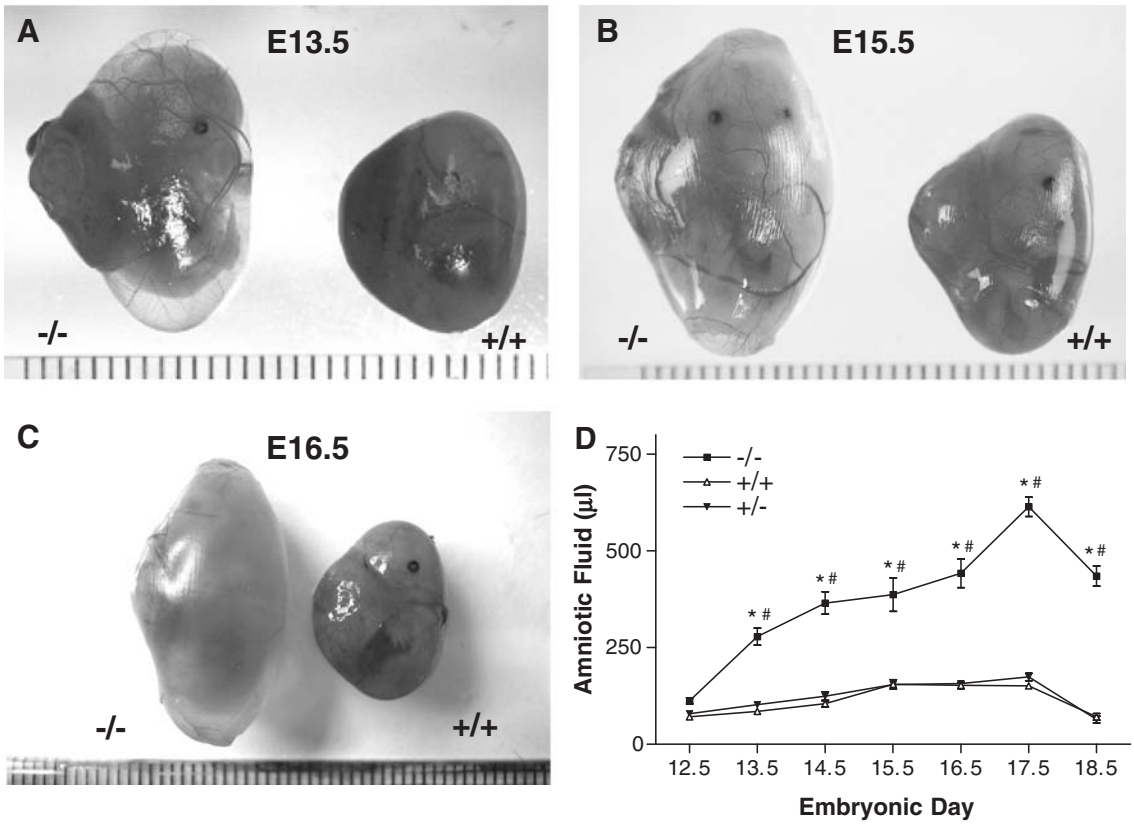


**Fig. 1.** Polyhydramnios in $Pkd1^{-/-}$ embryos. (**A–C**) $Pkd1^{-/-}$ embryos with massive polyhydramnios shown here inside the mother's uterine membrane at different stages of development in comparison with $Pkd1^{+/+}$ wild-type embryos: (**A**) E13.5, (**B**) E15.5 (**C**) E16.5. Bar = millimetre scale. (**D**) Time-course of amniotic fluid volume at each time point according to the *Pkd1* genotype ($n = 6$ to 19 embryos at each time point). The total amniotic fluid volume values were significantly higher in $Pkd1^{-/-}$ vs. $Pkd1^{+/+}$ and $Pkd1^{+/-}$ from E13.5 to E18.5. *$P < 0.0001$; #$P < 0.0001$, $Pkd1^{-/-}$ vs. $Pkd1^{+/-}$.

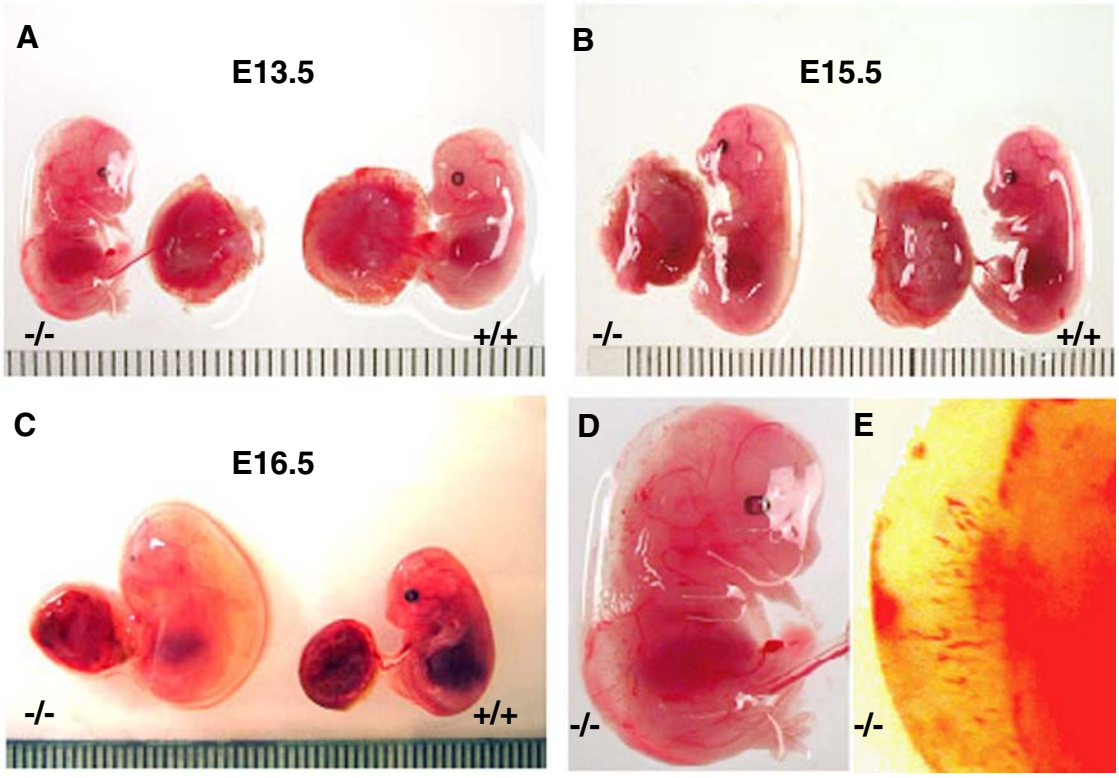


**Fig. 2.** Hydrops fetalis and vascular fragility in *Pkd1*$^{-/-}$ embryos. (**A–C**) *Pkd1*$^{-/-}$ embryos showed hydrops fetalis (generalized oedema, most visible on the back of the body) at E13.5 (A), E15.5 (**B**) and E16.5 (C). **D**. Focal haemorrhage in a *Pkd1*$^{-/-}$ embryo aged E13.5, demonstrating vascular fragility. **E**. High magnification of a *Pkd1*$^{-/-}$ embryo's back at E16.5, showing subcutaneous oedema and vascular fragility. Bar = millimetre scale.

embryos, with no detectable abnormalities in the labyrinth and the spongiotrophoblast (Suppl. Fig. 2).

### *Hydrops fetalis and vascular fragility in Pkd1*$^{-/-}$ *embryos*

In addition to polyhydramnios, *Pkd1*$^{-/-}$ embryos showed a typical phenotype of hydrops fetalis resulting in tissue edema, detectable from E13.5 and throughout gestation (Figure 2A–C). Edema of the back of the body caused a vertical shape, preventing *Pkd1*$^{-/-}$ embryos from being curved as the wild-type embryos. Moreover, the *Pkd1*$^{-/-}$ embryos showed areas of focal haemorrhage in different regions of the body, such as the neck and abdomen (Figure 2D, E). The vascular rupture could be observed as early as E13.5 and continuing to E18.5.

### *Pattern of cystogenesis in the Pkd1*$^{-/-}$ *embryonic kidneys*

Histological analysis (Figure 3) showed that the renal cysts in *Pkd1*$^{-/-}$ embryos were first detected at E15.5 (Figure 3B), consistent with the other *Pkd1*-mutant mouse models. The first cysts at E15.5 were located in the internal area of the kidney, and a large majority of them were glomerular cysts characterized by the cystic enlargement of the Bowman space and the presence of glomerular tufts (Figure 3F and Figure 4). The glomerulocystic phenotype was only observed for glomeruli located in the deep medulla zone, whereas superficial glomeruli located in the cortex among comma and S-shaped bodies were non-cystic (Figure 4A). At high magnification, the cysts arise from the dilation of the Bowman capsule, with flattened cells and discontinuous cell lineage. The podocytes, typically organized in a crown surrounding the capillaries in the young glomeruli, showed no abnormalities (Figure 4B). Immunostaining for the endothelial marker CD31/PECAM-1 identified the normal glomerular vascularization in these sections (Figure 4C, D).

From E16.5, cystogenesis progressed from the medulla towards the cortical area, still involving glomeruli as well as tubular segments (Figure 3G). By E18.5 the cysts were detected in all areas of the kidney (Figure 3H). Quantification revealed that glomerular cysts accounted for ~65% (128/197) of the total number of cysts at E15.5 and ~45% (110/246) at E16.5 (Table 2). Apart from atrophic lesions of the glomerular tuft, which were observed from E16.5, there was no evidence for fibrosis, inflammatory infiltrate, tubular casts or epithelial hyperplasia in the *Pkd1*$^{-/-}$ kidneys. Of note, even in mutant embryos, nephrogenesis continued on until birth in the external cortex.

### *Segmental origin of the cysts in Pkd1-mutant kidneys*

To further characterize the segmental origin of the cysts, serial sections of *Pkd1*$^{-/-}$ kidneys were stained with megalin, a multi-ligand receptor that is specifically expressed in PT cells [16], and DBA lectin, a marker of the distal convoluted tubule and the collecting duct [17] (Figure 5). No cyst was observed at E14.5, whereas developing tubular

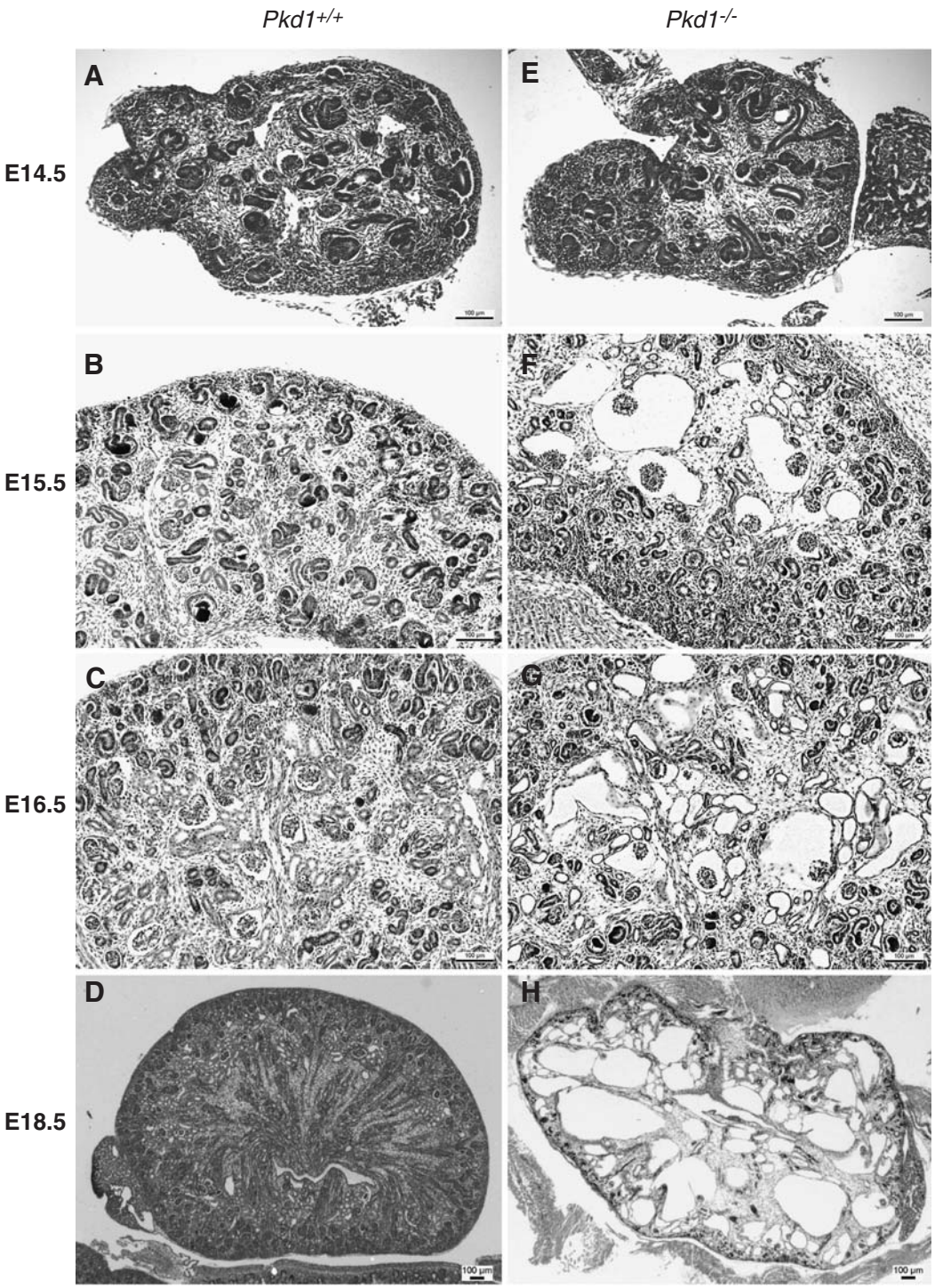


**Fig. 3.** Stages of renal development in *Pkd1* embryos. Representative sections (hematoxylin and eosin staining) of $Pkd1^{+/+}$ (**A–D**) and $Pkd1^{-/-}$ (**E–H**) embryonic kidneys at different stages of development. Progressive cyst formation, starting from glomeruli and later extending to tubular segments, is observed in $Pkd1^{-/-}$ kidneys beginning at E15.5 (**F–H**). Bar = 100 µm.

profiles positive for megalin or DBA lectin were detected (Figure 5A, E). At E15.5, some of the cysts at the corticomedullary junction were stained with megalin, whereas no cysts were stained with DBA lectin (Figure 5B, F). At E16.5, a fraction of cysts located in medulla and corticomedullary area were positive for megalin (70/246, 28%), or less frequently, DBA lectin (42/246, 17%) (Figure 5C, G; Table 2). There was no cross-reactivity between megalin and DAB lectin in the same cyst (Figure 5B–H).

Further analyses showed that the staining for megalin, which was strictly apical in wild-type and non-cystic tubule profiles, was less polarized, diffusely increased or

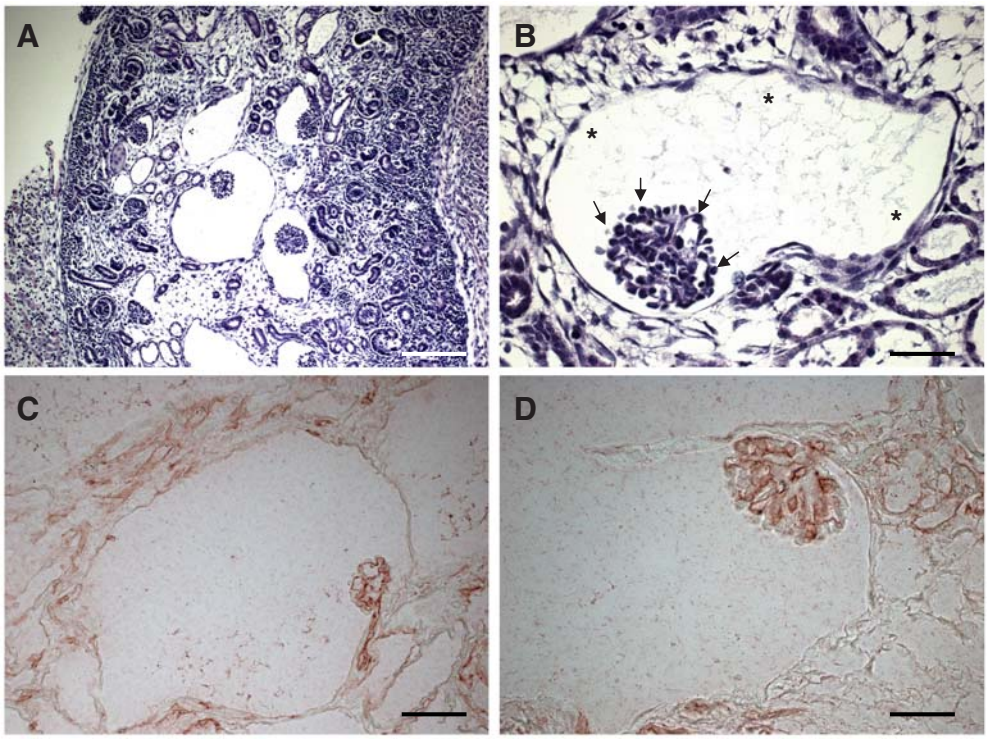


**Fig. 4.** Glomerular cysts in *Pkd1*-null embryos. (**A, B**) At E15.5, a typical picture of glomerulocystic kidney disease was observed in $Pkd1^{-/-}$ embryos. The glomerulocystic phenotype was only observed for glomeruli located in the deep medulla zone, whereas superficial glomeruli located in the cortex among comma and S-shaped bodies were non-cystic (**A**). At high magnification (**B**), the cysts arise from the dilation of the Bowman capsule, with flattened cells and discontinuous cell lineage (asterisk). The podocytes, typically organized in a crown surrounding the capillaries in the young glomeruli (arrows), showed no abnormalities. The start of early proximal tubules could be seen in some glomerular cysts, without tubular dilation at E15.5. Immunostaining for CD31 (**C–D**) was used as a marker of glomerular vascularization in cysts identified at E18.5. Bar = 80 μm (A); 20 μm (B, D); 40 μm (C).

**Table 2.** Segmental origin of the cysts in *Pkd1*-null embryonic kidneys

| Age | Kidney sections (*n*)[a] | Glomerular cysts (*n*) | Megalin[b] | *n* | DBA lectin[b] | *n* | Undefined cysts (*n*) | Total cysts (*n*) |
|---|---|---|---|---|---|---|---|---|
| E13.5 | 8 | 0 | ++ | 0 | + | 0 | 0 | 0 |
| E14.5 | 8 | 0 | ++ | 0 | ++ | 0 | 0 | 0 |
| E15.5 | 10 | 128 | ++ | 54 | ++ | 0 | 15 | 197 |
| E16.5 | 8 | 110 | ++ | 70 | ++ | 42 | 24 | 246 |

[a]These sections were obtained from four to five embryos.
[b]Staining intensity: +, weak positive staining; ++, strong positive staining.

even absent in the epithelial cells lining PT cysts in the $Pkd1^{-/-}$ kidneys (Figure 6). The glomerular cysts were unstained, except for some megalin-positive PT cells identified at the urinary pole of the Bowman capsule. Only ~10% of the tubular cysts were negative for both markers (Table 2). We could not obtain clear staining for AQP1 (PT marker), uromodulin (thick ascending limb marker) or AQP2 or calbindin (collecting duct markers) at any stage, even after antigen retrieval (data not shown). These data show that, in this *Pkd1*-null mouse model, the first renal cysts are detected at E15.5 in mesenchyme-originated tissues rather than ureteric bud-originated tissues, and that a majority of glomerular cysts is observed at E15.5 and E16.5.

### *Expression of Pkd1 and polycystin-1 during mouse nephrogenesis*

We next investigated the pattern of *Pkd1* and polycystin-1 expression in the developing mouse (Figure 7). Using the β-galactosidase reporter gene, *Pkd1* expression was not detected in the pronephros or mesonephros prior to the development of the definitive metanephric kidney in the $Pkd1^{del17-21\beta geo\ +/-}$ mouse. From E13.5–E15.5, weak *Pkd1* expression was seen in the condensed mesenchyme surrounding the ureteric bud tips and weakly in some cells within the uncondensed mesenchyme but not in the ureteric bud tips themselves. *Pkd1* expression was also seen in endothelial cells migrating into the S-shaped

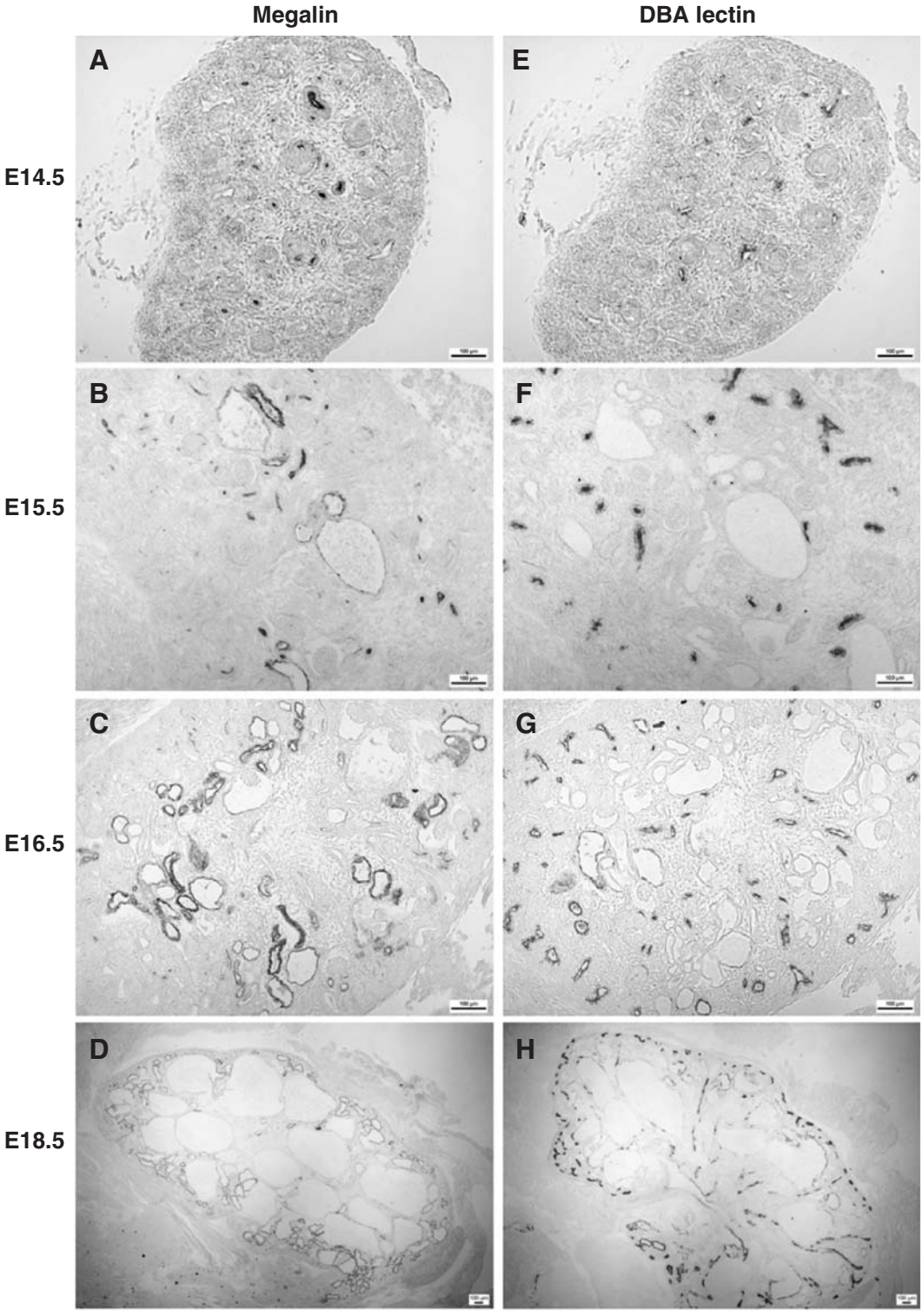


**Fig. 5.** Segmental origin of cysts in *Pkd1*$^{-/-}$ embryonic kidneys. Serial sections of *Pkd1*$^{-/-}$ embryonic kidneys at different stages of development stained with megalin, a marker of the proximal tubule (**A**–**D**), and DBA lectin, a marker of the distal tubule and collecting duct (**E**–**H**). Non-cystic tubule profiles are stained at E14.5, without cross-reactivity between the two markers (A, E). At E15.5, some cysts are stained with megalin (**B**), whereas DBA staining is still restricted to non-cystic tubules (**F**). At E16.5 and E18.5, some cysts are stained with megalin, whereas other cysts are positive for DBA lectin, indicating proximal vs. collecting duct origin respectively (**C**–D vs. **G**–H). There was no cross-reactivity between megalin and DAB lectin in the same cyst. Bar = 100 μm.

body to form the glomerulus. From E15.5, there was marked upregulation of *Pkd1* expression within the developing metanephros and in the glomerular parietal epithelium, differentiating PT and collecting ducts (Figure 7A, B). Vascular staining was also detected, whereas early nephron precursors and ureteric bud tips in the peripheral

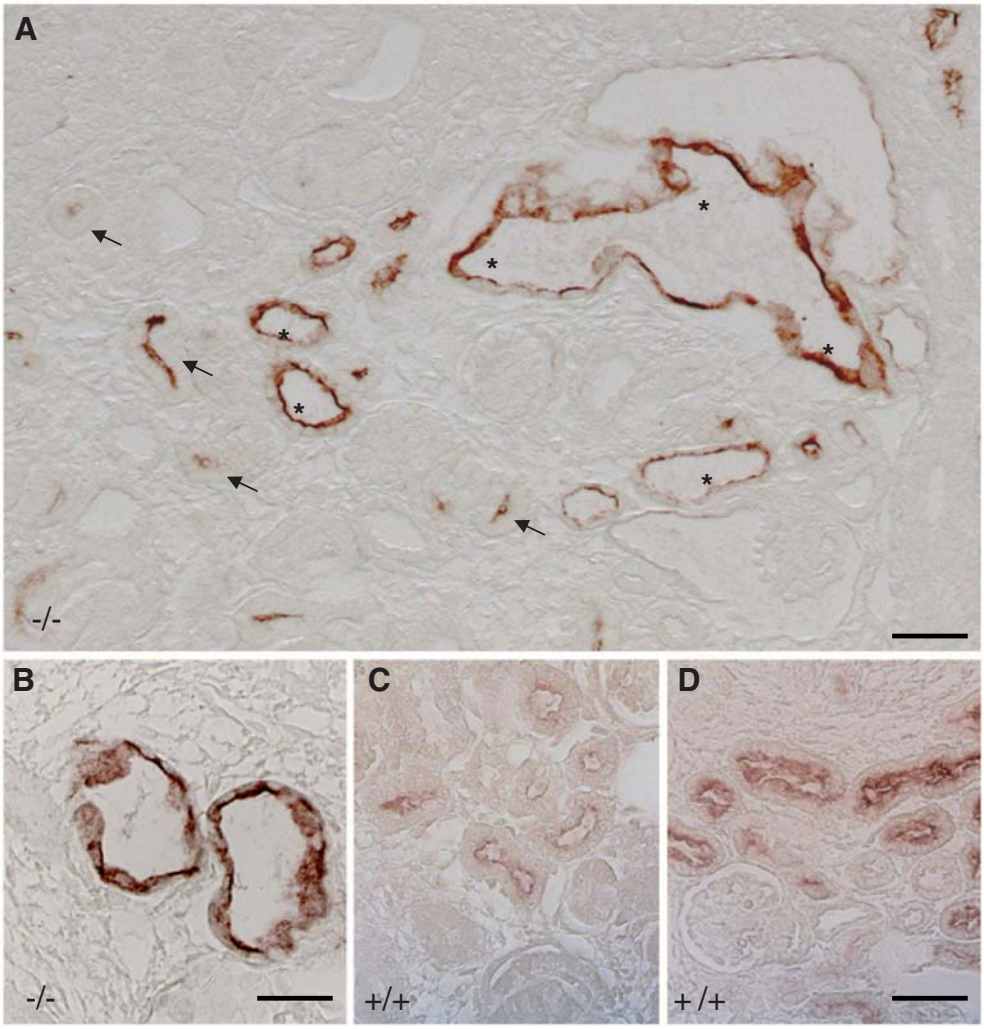


**Fig. 6.** Distinct patterns of megalin immunoreactivity in *Pkd1* kidneys. Immunolocalization of the multi-ligand receptor megalin in representative sections of $Pkd1^{-/-}$ (**A**, **B**) and $Pkd1^{+/+}$ (**C**, **D**) kidneys at E16.5 (A–C) and E18.5 (D). A distinct and well-delineated apical staining for megalin is observed in non-cystic proximal tubule profiles of $Pkd1^{-/-}$ kidneys (**A**, arrows), similar to that observed in wild-type kidneys (C, D). This pattern contrasts with the increased reactivity, loss of polarity and even loss of expression observed in the flattened cells lining adjacent cystic profiles (A, asterisks; B, higher magnification). Bar = 40 μm (A, C, D); 20 μm (B).

cortex remained negative. Immunostaining for polycystin-1 (anti-LRR antibodies) detected a specific signal in the glomerular parietal epithelium and in the PT epithelial cells in E15.5 $Pkd1^{+/+}$ kidneys (Figure 7E–F), whereas no specific staining was observed in the corresponding regions of $Pkd1^{-/-}$ kidneys (Figure 7G). This staining pattern was confirmed (although with a higher background) when using the 7E12 antibody against polycystin-1 (data not shown).

### *Massive loss of solutes and increased cAMP levels in AF*

The AF collected from E13.5 to E16.5 was analyzed in order to calculate the amount of solute excreted in each genotype (Figure 8). The $Pkd1^{-/-}$ embryos were characterized by a significantly higher excretion of sodium and glucose from E13.5 through E16.5 (Figure 8A, B). Time-course analysis of the LMW protein CC16 in the AF of the wild-type embryos revealed a progressive decrease from E13.5 to E16.5, followed by an abrupt rise at E17.5 as a marker of foetal lung growth, as previously described [15]. By contrast, the CC16 excretion progressively increased from E13.5 to E16.5 in the $Pkd1^{-/-}$ embryos, being significantly higher than the wild-type at E15.5 and E16.5 (Figure 8C). Furthermore, there was a progressive increase in the cAMP excreted in the AF of *Pkd1*-null embryos at E14.5, and even further at E15.5, which was concurrent with cystogenesis (Figure 8D). These data show that deletion of *Pkd1* is associated with a substantial loss of solutes, including the LMW protein CC16 before the onset of lung growth, and increased cAMP levels in the AF.

## Discussion

In this study, we have analysed the consequences of *Pkd1* deletion on the time-course and pattern of cy-

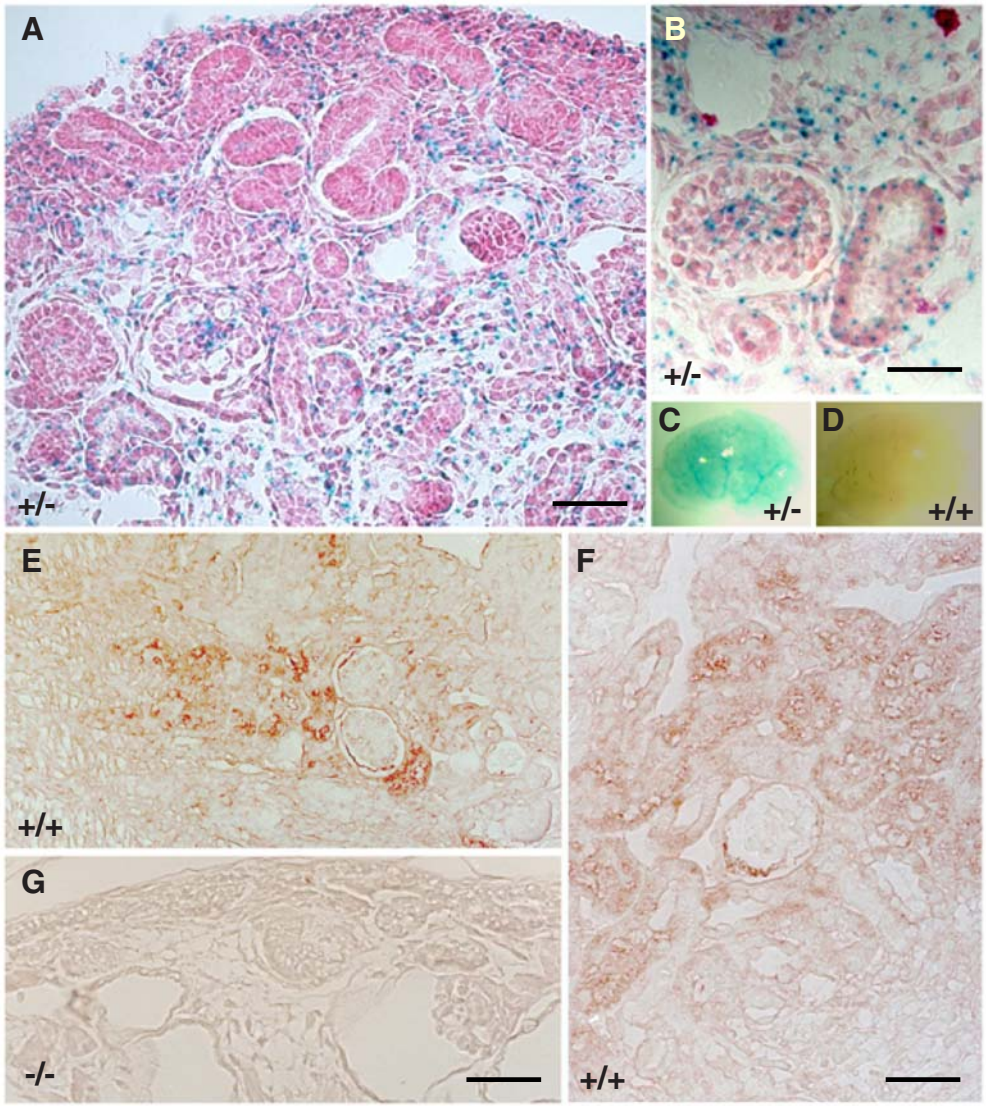


**Fig. 7.** Expression of *Pkd1* and polycystin-1 in the developing mouse kidney. (**A–D**) LacZ staining for *Pkd1* expression in $Pkd1^{del17\text{-}21\beta geo\ +/-}$ mice. The expression of *Pkd1* in the glomerular parietal epithelium and in proximal and more distal tubule epithelial cells is seen at low magnification (panel A, E16.5). Note that the renal capsule is also a site of *Pkd1* expression. The glomerular and proximal tubular expression is detected as early as E15.5 (panel **B**). Panels **C** (+/−) and D (+/+) are positive and negative whole mount controls for the lacZ staining, respectively. (**E–G**) Immunostaining for polycystin-1 (anti-LRR antibodies) in E15.5 *Pkd1* kidneys. A clear signal is observed in the glomerular parietal epithelium and in the proximal tubule epithelial cells of $Pkd1^{+/+}$ kidneys (panels E and **F**). No specific staining is observed in the corresponding region of a *Pkd1* KO kidney (panel G). Bar = 30 μm (A, F); 20 μm (B); 40 μm (E, G).

stogenesis, the structure of the placenta and the AF volume and composition in mouse embryos. The *Pkd1*-null embryos start to die at E13.5, with consistent features including hydrops fetalis, renal cysts and vascular fragility, in absence of placental abnormalities. This *Pkd1*-null model is characterized by an early polyhydramnios, with an excessive loss of various solutes, including cAMP, in the AF. These features precede the development of renal cysts, which are first detected in glomeruli and PT, and later in distal nephron segments.

Nephrogenesis in mouse and man is characterized by a repetitive and reciprocal induction between the ureteric bud and the metanephric mesenchyme, resulting in the formation of mature kidneys before birth. The first cysts in $Pkd1^{-/-}$ embryonic kidneys are observed at E15.5, starting in mesenchyme-originated tissues, with the majority of cysts arising from mature glomeruli and a significant proportion from the PT segments as indicated by positive megalin staining. These events are reflected by a rise in embryonic lethality at E15.5. The segmental cystogenesis in our model is consistent with the pattern of *Pkd1* expression in the mouse as reported by Boulter *et al.* [5] and further detailed here using lacZ staining on developing kidneys from $Pkd1^{del17–21\beta geo\ +/-}$ mice (Figure 7). In agreement with *in situ* hybridization data [18], these studies show that *Pkd1* expression is limited during early nephrogenesis, with weak expression in the mesen-

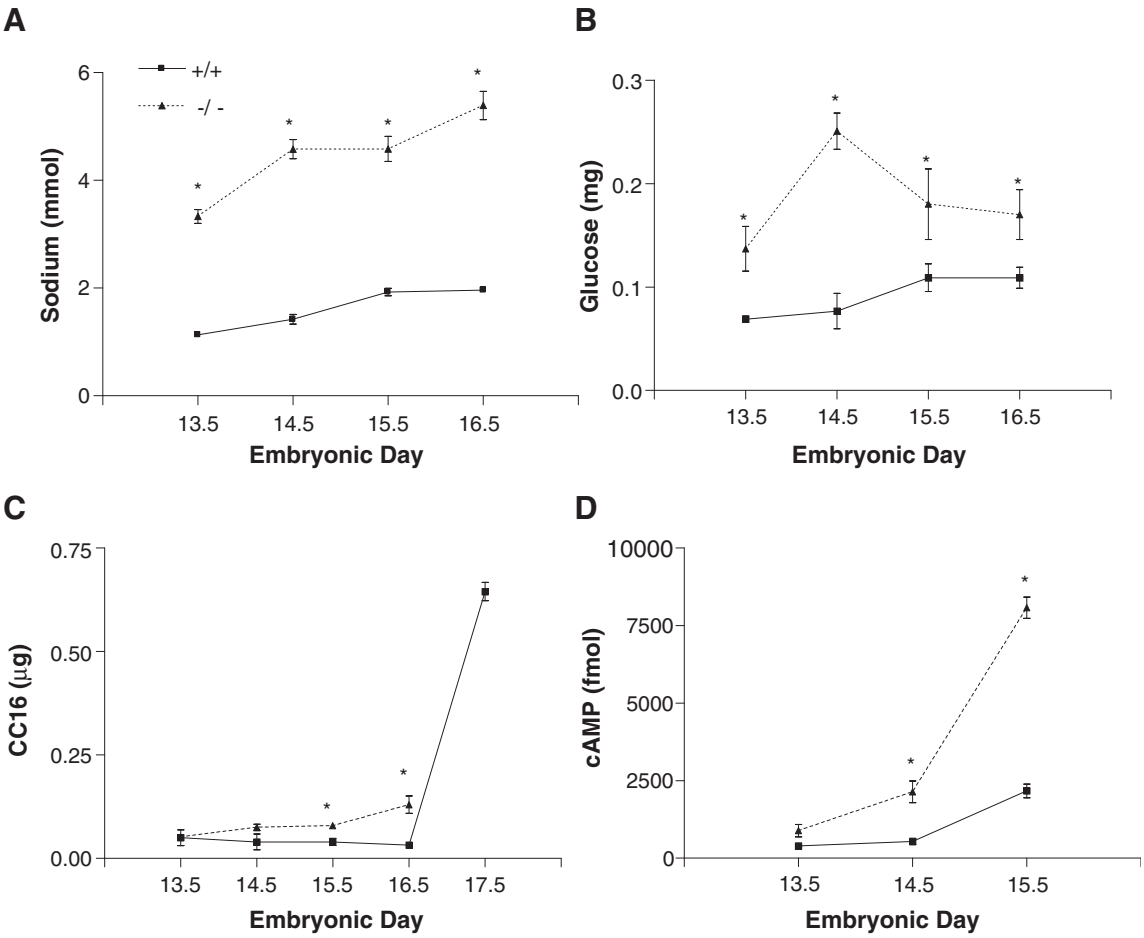


**Fig. 8.** Time-course of solute excretion in the amniotic fluid of *Pkd1* embryos. Total excretion of sodium (**A**), glucose (**B**), CC16 (**C**) and cAMP (**D**) in the amniotic fluid of $Pkd1^{+/+}$ vs. $Pkd1^{-/-}$ embryos. The excretion of sodium (A) and glucose (B) was higher in $Pkd1^{-/-}$ embryos during the course of embryogenesis (*$P < 0.0001$, $n = 4$ to 15 at each embryonic day). The excretion of CC16 progressively decreased from E13.5 to E16.5 in the wild-type embryos, followed by an abrupt rise at E17.5 due to foetal lung growth. By contrast, the CC16 excretion progressively increased from E13.5 to E16.5 in $Pkd1^{-/-}$ embryos, being significantly higher than the wild-type at E15.5 and E16.5 (no viable embryo at E17.5) (C). The excretion of cAMP (D) was significantly higher in $Pkd1^{-/-}$ vs. $Pkd1^{+/+}$ embryos at E14.5 and further at E15.5 (*$P < 0.02$, #$P < 0.0001$, $n = 4$ at each embryonic day).

chyme and no expression in the ureteric bud. From E15.5, *Pkd1* expression increased dramatically in induced mesenchymal cells, including maturing PT, and subsequently, more distal nephron segments [5]. The initial and intense expression of *Pkd1* in glomerular parietal epithelium and PT is in line with the first cystic lesions observed here and in the $Pkd1^{del34/del34}$ mice [6]. Glomerular cysts have also been reported in the $Pkd1^{L/L}$ mouse model characterized by a severe phenotype including vascular defect leading to haemorrhagic lesions and lethality by E15.5 [7]. Furthermore, glomerular cysts were detected in the adult kidneys from two models of transgenic mice overexpressing normal *PKD1* [19] or *Pkd1* [20], suggesting the importance of a precise regulation of polycystin-1 expression for normal glomerular maturation and tubulogenesis.

Hydrops fetalis, a term used to describe foetuses with generalized oedema and cavity effusions, is observed in the $Pkd1^{-/-}$ embryos like in the majority of *Pkd1* KO mice thus far [5,7–9]. Fluid balance in the foetus integrates placental fluid transfer, capillary filtration, swallowing, lung secretion and urine production [21]. Accordingly, many features observed in the *Pkd1* mice may explain an interstitial fluid accumulation, including abnormal vascular permeability, cardiac malformations and impaired renal function. The $Pkd1^{-/-}$ embryos investigated here show a significant polyhydramnios, consistently observed from E13.5 and throughout development. By contrast, the AF volume is stable across gestation in both wild-type and heterozygous *Pkd1* mice, followed by a sharp decrease at E18.5, similar to the human and mouse situation [21,22]. In addition to our model, polyhydramnios has only been reported in another *Pkd1*-null mouse [8]. Polyhydramnios may result from salt-losing tubulopathies or increased foetal urine output secondary to diabetes insipidus [23]. The AF fluid analyses demonstrated a massive loss of sodium and glucose in the $Pkd1^{-/-}$ embryos starting at E13.5, i.e. 2 days before cystogenesis. There is also an increased excretion of the LMW protein CC16 at E15.5 and E16.5 in the AF of *Pkd1*-mutant embryos, before

the sharp increase due to lung maturation [15]. CC16 is typically reabsorbed by PT cells through the multi-ligand megalin receptor pathway [16]. We showed previously that the polarized expression of essential components of the PT endocytic apparatus (e.g. ClC-5 and vacuolar $H^+$-ATPase subunits) is acquired at E15.5 [24]. The co-expression of these molecules—including megalin as reported here—immediately after the onset of glomerular filtration [25] suggests an early maturation of PT function. Together with the abnormal megalin expression observed in PT-derived cysts, the increased excretion of CC16 in the AF suggests that PT maturation may be altered in the *Pkd1*$^{-/-}$ mice. In that respect, it is interesting to note that an abnormal excretion of PT markers is an earliest functional defect in patients with ADPKD [11].

Placental malformations may also cause abnormal fluid balance in embryos. It has been suggested that abnormalities of the placental labyrinth layer, detected from E11.5, may cause *Pkd1*$^{-/-}$ foetal death [12]. By contrast, our morphometry analysis did not detect abnormalities in the four placental compartments, including the labyrinth layer (Suppl. Fig. 2). Thus, gross placental abnormalities cannot explain the hydrops fetalis and polyhydramnios observed at E13.5 in our model. As the phenotype of *Pkd1* mice is notoriously dependent on the genetic background, one could speculate that differences in placenta morphology could reflect the different background (129Sv vs. C57BL/6J, respectively) of the models.

We observed increased cAMP levels in the AF of *Pkd1*$^{-/-}$ embryos at E14.5 and E15.5, concomitant to cystogenesis. A progressive increase in cAMP in the AF has been reported in normal human pregnancy [26], which could reflect the progressive increase in glomerular filtration and the maturation of PT and response to parathyroid hormone [27]. As glomerular filtration—and tubular maturation (see above)—start at E14.5 in mouse, the increased levels observed at both E14.5 and E15.5 in *Pkd1*-null embryos could reflect epithelial tubular production, in addition to the maternal origin or production by the amniotic membranes. Previous studies have shown that increased levels of cAMP could play a major role in cyst formation, through stimulation of fluid secretion and cell proliferation (reviewed in [2]). In two cystic models orthologous to human autosomal recessive PKD (PCK rat) and nephronophthisis (*pcy* mouse), and one cystic model orthologous to human ADPKD (*Pkd2*$^{-/tm1Som}$ mouse), increased renal cAMP levels, paralleled with higher expression of AQP2 and arginine vasopressin (AVP) V2 receptor (V2R), have been reported [28–30]. Recently, Magenheimer *et al.* showed that embryonic kidney tubules from E13.5 to E15.5 could be stimulated by cAMP to form cyst-like structures of both proximal tubule and collecting duct origin, a process that is significantly enhanced in *Pkd1*$^{-/-}$ embryonic kidneys [31]. The mechanism responsible for increased cAMP production is probably multifactorial, involving the interaction of circulating AVP with the V2R in the collecting duct, together with decreased intracellular calcium levels which can activate adenylyl cyclase 6 and/or inhibits phosphodiesterase 1 [2]. The involvement of the V2R pathway has been substantiated by the effects of V2R antagonists in various genetic models of PKD, with decreased renal cAMP levels associated with slowed cyst and renal enlargement and improved renal function, motivating a multicentric trial to test the efficacy of a selective V2R antagonist in ADPKD patients [32].

The effects of V2R antagonists on cAMP generation and the cystic phenotype in ADPKD are based on the assumption that ADPKD cysts are predominantly of collecting duct origin. However, the deletion of *Pkd1* in this mouse model is associated with predominant glomerular cysts at E15.5, followed by the development of (megalin-positive) PT cysts and later by collecting duct cysts. Accordingly, the V2R/AQP2 pathway, which is restricted to the collecting duct and not expressed in the glomerular parietal epithelium or in the PT, is not necessary for cyst development at least in this model. These findings in *Pkd1* mice may also yield insights into the segmental origin of cysts in human ADPKD. In the developing human kidney, high *PKD1* expression first appears in differentiated PT starting from their glomerular origin and later in the distal nephron and the ureteric bud branches [4]. Glomerular cysts have been reported in patients with ADPKD [33], including in a severe childhood case associated with a *PKD1* deletion [34]. Earlier analyses of cyst fluid composition, electric properties and immunoreactivity for segmental markers (including AQP1 and aminopeptidase) have identified a significant number of cysts of PT origin co-existing with collecting duct cysts in end-stage kidneys of ADPKD patients [3,35].

In conclusion, we show that the deletion of polycystin-1 in this mouse model is reflected by polyhydramnios and a massive loss of solutes, including cAMP, in the AF. These changes precede the development of renal cysts, first detected in glomeruli and PT. These features give insights into the role of polycystin-1 in renal development, the mechanisms of cystogenesis and the tubular alterations encountered in ADPKD.

## Supplementary data

Supplementary data are available online at http://ndt.oxfordjournals.org

*Acknowledgements.* The authors are grateful to Y. Cnops, H. Debaix, X. Dumont, K. Parreira and L. Wenderickx for excellent assistance, and Profs. A. Bernard, JP. Cosyns, A. Ong, Y. Pirson, A. Woolf and J. Zhou for helpful discussions. These studies were supported by the Belgian agencies FNRS and FRSM (3.4.592.06F), the 'Fondation Alphonse & Jean Forton', a Concerted Research Action (05/10-328), an Inter-university Attraction Pole (IUAP P6/05), the Programme d'excellence Marshall DIANE (Région Wallone), and the EUNEFRON (FP7, GA#201590) program of the European Community.

*Conflict of interest statement.* None declared.

## References


1. Pirson Y, Chauveau D, Devuyst O. Autosomal dominant polycystic kidney disease. *Oxford Textbook of Clinical Nephrology.* Oxford: Oxford University Press, 2005; 3rd Edition, 2304–2324
2. Torres VE, Harris PC. Mechanisms of disease: autosomal dominant and recessive polycystic kidney diseases. *Nature Clin Prac Neph* 2006; 2: 40–55
3. Devuyst O, Beauwens R. Ion transport and cystogenesis: the paradigm of autosomal dominant polycystic kidney disease. *Advances in Nephrology.* St. Louis: Mosby, 1998; 28439–478
4. Chauvet V, Qian F, Boute N *et al*. Expression of PKD1 and PKD2 transcripts and proteins in human embryo and during normal kidney development. *Am J Pathol* 2002; 160: 973–983
5. Boulter C, Mulroy S, Webb S *et al*. Cardiovascular, skeletal, and renal defects in mice with a targeted disruption of the Pkd1 gene. *Proc Natl Acad Sci USA* 2001; 98: 12174–12179
6. Lu W, Peissel B, Babakhanlou H *et al*. Perinatal lethality with kidney and pancreas defects in mice with a targetted Pkd1 mutation. *Nat Genet* 1997; 17: 179–181
7. Kim K, Drummond I, Ibraghimov-Beskrovnaya O *et al*. Polycystin 1 is required for the structural integrity of blood vessels. *Proc Natl Acad Sci USA* 2000; 97: 1731–1736
8. Lu W, Shen X, Pavlova A *et al*. Comparison of Pkd1-targeted mutants reveals that loss of polycystin-1 causes cystogenesis and bone defects. *Hum Mol Genet* 2001; 10: 2385–2396
9. Muto S, Aiba A, Saito Y *et al*. Pioglitazone improves the phenotype and molecular defects of a targeted Pkd1 mutant. *Hum Mol Genet* 2002; 11: 1731–1742
10. Nishio S, Hatano M, Nagata M *et al*. Pkd1 regulates immortalized proliferation of renal tubular epithelial cells through p53 induction and JNK activation. *J Clin Invest* 2005; 115: 910–918
11. Casal JA, Hermida J, Lens XM *et al*. A comparative study of three kidney biomarker tests in autosomal dominant polycystic kidney disease. *Kidney Int* 2005; 68: 948–954
12. Allen E, Piontek KB, Garrett-Mayer E *et al*. Loss of polycystin-1 or polycystin-2 results in dysregulated apolipoprotein expression in murine tissues via alterations in nuclear hormone receptors. *Hum Mol Genet* 2006; 15: 11–21
13. Ahrabi AK, Terryn S, Valenti G *et al*. Pkd1 haploinsufficiency causes a syndrome of inappropriate antidiuresis in mouse. *J Am Soc Nephrol* 2007; 18: 1740–1753
14. Ibraghimov-Beskrovnaya O, Dackowski WR, Let F *et al*. Polycystin: *in vitro* synthesis, *in vivo* tissue expression, and subcellular localization identifies a large membrane-associated protein. *Proc Natl Acad Sci USA* 1997; 94: 6397–6402
15. Halatek T, Hermans C, Broeckaert F *et al*. Quantification of Clara cell protein in rat and mouse biological fluids using a sensitive immunoassay. *Eur Respir J* 1998; 11: 726–733
16. Christensen EI, Brin H. Megalin and cubilin: multifunctional endocytic receptors. *Nat Rev Mol Cell Biol* 2002; 3: 256–266
17. Murata F, Tsuyama S, Suzuki S *et al*. Distribution of glycoconjugates in the kidney studied by use of labelled lectins. *J Histochem Cytochem* 1983; 31: 139–144
18. Guillaume R, D'Agati V, Daoust M *et al*. Murine Pkd1 is a developmentally regulated gene from morula to adulthood: role in tissue condensation and patterning. *Dev Dyn* 1999; 214: 337–348
19. Pritchard L, Sloane-Stanley JA, Sharpe JA *et al*. A human PKD1 transgene generates functional polycystin-1 in mice and is associated with a cystic phenotype. *Hum Mol Genet* 2000; 9: 2617–2627
20. Thivierge C, Kurbegovic A, Couillard M *et al*. Overexpression of PKD1 causes polycystic kidney disease. *Mol Cell Biol* 2006; 26: 1538–1548
21. Brace RA, Wolf EJ. Normal amniotic fluid volume changes throughout pregnancy. *Am J Obstet Gynecol* 1989; 161: 382–389
22. Cheung CY, Brace RA. Amniotic fluid volume and composition in mouse pregnancy. *J Soc Gynecol Investig* 2005; 12: 558–562
23. Kirshon B. Fetal urine in hydramnios. *Obstet Gynecol* 1989; 73: 240–242
24. Jouret F, Igarashi T, Gofflot F *et al*. Comparative ontogeny, processing, and segmental distribution of the renal chloride channel, ClC-5. *Kidney Int* 2004; 65: 198–208
25. Loughna S, Landels E, Woolf AS. Growth factor control of developing kidney endothelial cells. *Exp Nephrol* 1996; 4: 112–118
26. Yuen BH, Wittmann B, Staley K. Cyclic adenosine 3', 5'-monophosphate (cAMP) in pregnancy body fluids during normal and abnormal pregnancy. *Am J Obstet Gynecol* 1976; 125: 597–602
27. Webster SK, Haramati A. Developmental changes in the phosphaturic response to parathyroid hormone in the rat. *Am J Physiol* 1985; 249: F251–F255
28. Gattone VH, Xiaofang W, Harris PC *et al*. Inhibition of renal cystic disease development and progression by a vasopressin V2 receptor antagonist. *Nature Medicine* 2003; 9: 1323–1326
29. Torres VE, Xiaofang W, Qian Q *et al*. Effective treatment of an orthologous model of autosomal dominant polycystic kidney disease. *Nature Medicine* 2004; 10: 363–364
30. Wang X, Gattone V 2nd, Harris PC *et al*. Effectiveness of vasopressin V2 receptor antagonists OPC-31260 and OPC-41061 on polycystic kidney disease development in the PCK rat. *J Am Soc Nephrol* 2005; 16: 846–851
31. Magenheimer BS, St John PL, Isom KS *et al*. Early embryonic renal tubules of wild-type and polycystic kidney disease kidneys respond to cAMP stimulation with cystic fibrosis transmembrane conductance regulator/Na+, K+, 2Cl− co-transporter-dependent cystic dilation. *J Am Soc Nephrol* 2006; 17: 3424–3437
32. Torres VE, Bankir L, Grantham JJ. A case for water in the treatment of polycystic kidney disease. *Clin J Am Soc Nephrol* 2009; 4: 1140–1150
33. Verani RR, Silva FG. Histogenesis of the renal cysts in adult (autosomal dominant) polycystic kidney disease: a histochemical study. *Mod Pathol* 1988; 1: 457–463
34. Torra R, Badenas C, Darnell A *et al*. Autosomal dominant polycystic kidney disease with anticipation and Caroli's disease associated with a PKD1 mutation. *Kidney Int* 1997; 52: 33–38
35. Devuyst O, Burrow CR, Smith BL *et al*. Expression of aquaporins-1 and -2 during nephrogenesis and in autosomal dominant polycystic kidney disease. *Am J Physiol* 1996; 271: F169–F183


*Received for publication: 16.3.09; Accepted in revised form: 22.10.09*